

## Environmental friendly method for the extraction of coir fibre and isolation of nanofibre

Eldho Abraham<sup>a,b,d</sup>, B. Deepa<sup>b</sup>, L.A. Pothen<sup>b,\*</sup>, J. Cintil<sup>c</sup>, S. Thomas<sup>c</sup>, M.J. John<sup>d</sup>, R. Anandjiwala<sup>d</sup>, S.S. Narine<sup>a</sup>

<sup>a</sup> Trent Biomaterials Research Program, Trent University, Peterborough, Ontario, Canada

<sup>b</sup> Department of Chemistry, Bishop Moore College, Mavelikkara, Kerala, India

<sup>c</sup> School of Chemical Sciences, Mahatma Gandhi University, Kottayam 686 560, Kerala, India

<sup>d</sup> Fibres and Textiles Competence Area, CSIR, Materials Science and Manufacturing, PE, South Africa

### ARTICLE INFO

#### Article history:

Received 19 June 2012

Received in revised form

24 September 2012

Accepted 22 October 2012

Available online 30 October 2012

#### Keywords:

Coir fibre

Steam explosion

Extraction

Cellulose nanofibre

### ABSTRACT

The objective of this work was to develop an environmental friendly method for the effective utilization of coir fibre by adopting steam pre-treatment. The retting of the coconut bunch makes strong environmental problems which can be avoided by this method. Chemical characterization of the fibre during each processing stages confirmed the increase of cellulose content from raw (40%) to final steam treated fibres (93%). Morphological and dynamic light scattering analyses of the fibres at different processing stages revealed that the isolation of cellulose nano fibres occur in the final step of the process as an aqueous suspension. FT-IR and XRD analysis demonstrated that the treatments lead to the gradual removal of lignin and hemicelluloses from the fibres. The existence of strong lignin–cellulose complex in the raw coir fibre is proved by its enhanced thermal stability. Steam explosion has been proved to be a green method to expand the application areas of coir fibre.

© 2012 Elsevier Ltd. All rights reserved.

### 1. Introduction

The promising performance of cellulose nanofibres and their abundance encourages the utilization of agricultural waste residue, which acts as the main source of cellulose. In nature, a large number of plants and animals synthesize extra-cellular high-performance skeletal biocomposites consisting of a matrix reinforced by fibrous biopolymers (Mohanty, Misra, & Hinrichsen, 2000). Cellulose is a classical example where the reinforcing elements exist as whisker-like microfibrils that are biosynthesized and deposited in a continuous manner (Itoh & Brown, 1984). Coir fibre obtained from coconut husk is one of the major underutilized raw material which is composed of cellulose nanofibre which constitutes 32–43% of its dry weight (Arylmis, Jarusombuti, Fueangvivat, Bauchongkol, & White, 2011). Total world coir fibre production is 250,000 tonnes per year and out of it, 80% of the fibre is contributed by the coastal region of Asia (Hon, 1994). The raw fibres have been reported to be used in the field of polymer composite application (Geethamma, Thomas Mathew, Lakshminarayanan, & Thomas, 1998). Efforts are going on for exploring wider export markets for coir and coir products but still most of the raw coir fibre remain underutilized. Judged

from the increase in production and employment, the progress has been rather slow and exports in physical terms have remained mere or less static.

Another major issue is related to the pollution originated during the retting and processing of raw coir fibre (Narayanan, 1999). One of the striking features of southern India is the continuous chain of lagoons or backwaters existing along the coastal region. The backwaters support rich and diverse life forms and provide crucial nurseries for shrimps and fishes as well as habitat for oysters, clams and mussels which later enrich the ocean. The shallow fringes of the backwaters and the channels drawn from them are used for retting of coconut husk. It adversely affects the productivity of the backwaters and is harmful to marine fisheries. The retting process is brought about by the pectinolytic activity of micro organisms especially bacteria, fungi and yeasts degrading the fibre binding materials of the husk and liberating large quantities of organic matter and chemicals into the environment, including pectin, pentosan, tannins, polyphenols, etc. Consequently hydrogen sulphide, phosphate and nitrate contents increase while dissolved oxygen and community diversity of plankton decrease in the ambient waters during the retting process. Here we report a novel environmental friendly method to use the raw coir fibre as they exist in the coconut husk, and thereby avoiding the retting steps of the coir fibre.

In an earlier work, nanocellulose was prepared from banana fibres by steam explosion (Abraham et al., 2011). Coir husk is

\* Corresponding author. Tel.: +91 479 2301730.

E-mail address: [lapothen@gmail.com](mailto:lapothen@gmail.com) (L.A. Pothen).

another important source of cellulose. The coir fibre comprise mainly of cellulose, lignin and hemicellulose. The cellulose part is crystalline and the lignin part is completely amorphous in nature (Mohanty et al., 2000). Coir fibre industry mainly uses the fibre as it is obtained from the coconut fruit and no other extraction procedure has been reported yet. However, such separation is mandatory for its effective utilization in the current nanotechnological areas. The extracted lignin is a suitable source for renewable energy production. In this paper we report on a novel technique, steam explosion, for the separation of nanocellulose from coir fibre and there by expanding its application fields. In the various pre-treatment technologies for the isolation of nanocellulose fibres, steam explosion is an attractive choice. We used mild acids with low concentration which avoids toxicity. Since nanocellulose is a hot topic in the current research field (Abraham et al., 2011; Zimmermann, Pohler, & Geiger, 2004; Goetz, Mathew, Oksman, Gatenholm, & Ragauskas, 2009), and its generation by a low cost method by a green pathway makes this work more important in this current environmental scenario.

## 2. Experimental

### 2.1. Materials

Coconut husk which is the principle source for the coir fibre were collected from locally available waste bunch of the coconut fruit. All the various chemicals used for extraction of the fibre are  $\text{NaClO}_2$ ,  $\text{NaOH}$  and oxalic acid are of analytical grade obtained from Nice chemicals, Cochin, India. The chemicals used are in mild concentration to accomplish the environmental friendliness.

### 2.2. Chemical analysis of the fibres

Chemical constituents of fibres were determined according to ASTM standards.  $\alpha$ -cellulose (ASTM D 1103-55T), hemicellulose (ASTM D 1104-56), lignin (ASTM D 1106-56), Moisture content (ASTM D 4442-92). The cellulose, hemicelluloses, lignin and moisture content of the fibre in the untreated raw, steam exploded and acid hydrolysed stages of the coir fibre were determined.

### 2.3. Methods for the isolation of nano cellulose from raw fibres

#### 2.3.1. Alkali treatment of the fibre

The alkali treatment will make the coir fibre more exposure to bleaching and acid hydrolysis. The optimum caustic soda treatment is both a very effective surface modification and a low cost surface treatment for coir fibres. Locally available coconut husk were cut it into pieces and subjected for treatment. Coir fibres were soaked in 2% caustic soda and placed for six hours at a temperature of 25 °C.

#### 2.3.2. Steam explosion of the alkali treated fibre

A laboratory autoclave which can work with 137 Pa (20 lbs) pressure was used for steam treatment. Steam explosion technique was applied on the alkali treated fibre for one hour. Steam pre-treatment was performed by loading the lignocellulosic material directly into the steam gun and treating it with high pressure steam at temperatures within 100–150 °C. The term used 'steam exploded fibre' means the alkali treatment followed by steam exploded coir fibre.

#### 2.3.3. Bleaching of the steam exploded fibre

Alkali treated and steam exploded samples are then subjected to bleaching. The bleaching treatment with sodium chlorite ( $\text{NaClO}_2$ ) solution (pH 2.3) for 1 h at 50 °C was performed to remove the remaining lignin. In the bleaching step, the absence of elemental

chlorine which causes strong environmental problems is accomplished by using  $\text{NaClO}_2$ .

#### 2.3.4. Acid treatment followed by steam explosion

The bleached sample is then subjected to mild acid treatment. 5% oxalic acid was used for the acid hydrolysis followed by second step of steam explosion for one hour. A pressure of 137 Pa (20 lbs) was used, followed by sudden release of pressure. The fibres were then washed thoroughly by water and then subjected to mechanical stirring followed by sonication.

### 2.4. Fourier transform-infra red spectroscopy (FTIR)

The FTIR spectra were recorded on an attenuated total reflection fourier transform infrared (ATR-FTIR) instrument (Nicolet 5700, Thermo Electron Corp., USA) in the range of 400–4000  $\text{cm}^{-1}$  with a resolution of 4  $\text{cm}^{-1}$ . The samples were ground into powder by a fibre microtome and then blended with KBr followed by pressing the mixture into ultra-thin pellets.

### 2.5. X-ray diffraction technique (XRD)

X-ray equatorial diffraction profiles of the fibres were collected by a JEOL diffractometer, Model JDX 8P, using  $\text{CuK}\alpha$  radiation at the operating voltage and current of 30 kV and 20 mA, respectively. The diffraction intensities were recorded between 2 and 80° ( $2\theta$  angle range).

### 2.6. Scanning electron microscopy (SEM)

Morphological analysis of untreated and steam exploded fibres were done by scanning electron microscopy. SEM micrographs of fibre surface were taken using a scanning electron microscope model JEOL JSM-35 C and Cambridge 250 MK<sub>3</sub> stereo scan operated at 10–20 kV. Prior to SEM evaluation, the samples were coated with gold for 5 minutes by means of a plasma sputtering apparatus.

### 2.7. Scanning probe microscopy (SPM)

The morphological study of the final nano cellulose fibrils were done by scanning probe microscopy. The scanning probe microscopy images of the nano fibres were made with a Multi-mode SPM (Veeco Inc., Santa Barbara, USA) with a Nanoscope IV controller in tapping mode. A dilute solution of nano dispersion which was sonicated just before the experiment was conducted.

### 2.8. Dynamic light scattering (DLS) and zeta potential

The particle sizing of nanocellulose dispersion in water was recorded by dynamic light scattering (DLS) system Inc., Santa Barbara, CA, USA. The principle of the DLS is based on the illumination of the sample by a laser beam followed by detection of the resultant fluctuations of the scattered light at a known scattering angle  $\theta$  by a fast photon detector.

The concentration of the solution was 0.1 g of nanocellulose dispersed by sonication in 1 litre of water. Run time of the experiment was 5–7 min. The measurements were performed with an angle of 160° by using laser (4 mW) and the wavelength of the scattering light used was 639 nm and the count rate was 284 KHz. The temperature of the system was 20 °C. The channel width was 200.0  $\mu\text{s}$  and the index of refractive was 1.347. Zeta potential measured as function of concentration of original aqueous coir cellulose suspension in 0.1 mM KCl electrolyte.

**Table 1**  
Constituents of the fibres in different stages.

	Cellulose (%)	Lignin (%)	Hemicellulose (%)	Moisture content (%)
Raw coir fibre	39.3 ( $\pm 4$ )	49.2 ( $\pm 5$ )	2 ( $\pm 0.5$ )	9.8 ( $\pm 1$ )
Alkali treated fibre	50.5 ( $\pm 3$ )	38.8 ( $\pm 4$ )	<1	10.3 ( $\pm 1$ )
Steam expl. fibre	57.4 ( $\pm 3$ )	30.9 ( $\pm 3$ )	–	8.8 ( $\pm 1$ )
Bleached fibre	88.3 ( $\pm 3$ )	0.3 ( $\pm 0.1$ )	–	8.5 ( $\pm 1$ )
Acid hydro. fibre	93.7 ( $\pm 2$ )	–	–	8.1 ( $\pm 0.5$ )

## 2.9. Thermo gravimetric analysis (TGA)

TGA analyses were carried out using a Mettler TG 50 module attached to a Mettler TC 11 4000 thermal analyzer (Switzerland). The thermal analyses were done in a nitrogen atmosphere under a flow rate of 100 mL/min using an alumina crucible with a pinhole. An average mass of 10 mg of the sample with a constant heating rate of 10 °C/min was maintained from room temperature to 700 °C.

## 3. Results and discussions

### 3.1. Chemical analysis of the fibres

Table 1 describes the chemical composition of the coir fibres at different processing stages as well as the moisture content. Chemical constituents of fibres were determined according to ASTM standards described in the experimental section. The raw coir fibre is mainly composed of cellulose (~40%), lignin (~45%) and other components. Upon alkali treatment, the lignin starts to dissolve out and increases the relative percentage of cellulose components. It is clearly demonstrated in the data presented in the table. The fine structure of cellulose materials is composed of crystalline and amorphous regions. The amorphous regions easily absorb chemicals such as dyes and resins, whereas the compactness of the crystalline regions makes it difficult for chemical penetration (Klemm et al., 2006). The alkali treatment of the coir fibres may involve the removal of the surface impurities, the swelling of the crystalline region, and alkalinisation of the peripheral hydroxyl groups. The common trend from the observation is the gradual decrease of amorphous components like lignin and hemicellulose from raw fibre to bleached fibre. The lignin will react with NaClO<sub>2</sub> and an oxidative fragmentation of lignin takes place and some part of lignin will dissolve out as lignin chloride. The percentage increase of the cellulose component (39.3–93.7%) and decrease of the lignin components (49.2–0.3%) with each processing steps are the main observation.

Moisture content shows an increase from raw to alkali treated fibre and then gradually decreases. During alkali treatment, the swelling of the fibre takes place, which promote the absorption of moisture by capillary action. The alkali treatment of the fibre will lead to the swelling which facilitate the breakdown during acid hydrolysis. During every processing step there is an increase in the percentage of crystalline cellulose content. Since most hydroxyl groups in the final stage are bonded by intra and inter molecular hydrogen bonding, moisture absorption decrease.

### 3.2. FT-IR analysis

Fig. 1 gives the FT-IR spectrum of coir fibre at different processing stages. As discussed in chemical analysis, the main components in the coir fibre are cellulose, hemicellulose and lignin. These three components are mainly composed of esters, aromatic ketones and alcohols, with different oxygen-containing functional groups. Erdtman, Klemm and Oh have reported on the infrared spectra of cellulose, hemicellulose and lignin (Erdtman, 2003; Klemm, Philipp, Heinze, Heinze, & Wagenknecht, 2004;

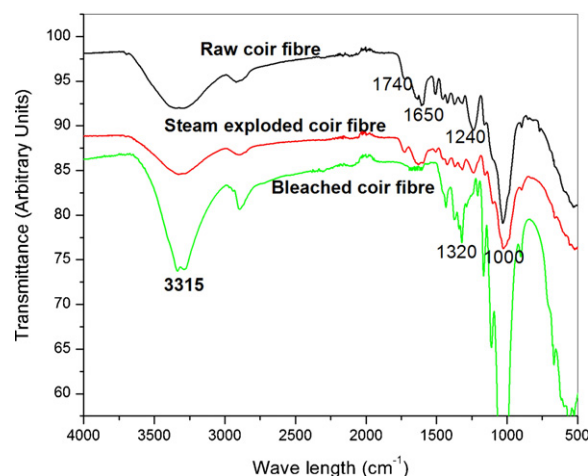


Fig. 1. FTIR spectra of coir fibre.

Klemm et al., 2006; Oh, Yoo, Shin, & Seo, 2005). Lignin present in the coir fibre gives characteristic peaks at 1240, 1650 and 1740 cm<sup>-1</sup> corresponding to the aromatic skeletal vibration and carbonyl group. It is clear from the spectra that these three peaks are completely absent in the bleached fibre. The peak present at 1650 cm<sup>-1</sup> in the spectrum corresponding to the raw fibres is due to the presence of C=O linkage, which is a characteristic group of lignin and at 1740 cm<sup>-1</sup> is due to hemicellulose. Another possibility is that carboxyl or aldehyde absorption could be arising from the opened terminal glycopyranose rings or oxidation of the C–OH groups. Alkali treatment reduces hydrogen bonding due to removal of the hydroxyl groups by reacting with sodium hydroxide (Reddy & Yang, 2005). This results in the decrease of the –OH concentration, evident from the decreased intensity of the peak between 3300 and 3320 cm<sup>-1</sup> bands compared to the untreated fibre (Lojewska, Miskowicz, Lojewski, & Pronienwicz, 2005). Since the bleached fibre is crystalline cellulose, its spectra gives the transmittance of the three hydroxyl groups. The exposed hydroxyl group of the cellulose is clearly seen from the increased intensity of the 3315 cm<sup>-1</sup> peak. The three hydroxyl functional group present in the cellulose structure is primarily responsible for this peak in addition to aromatic hydroxyl groups present in the lignin and the water absorbed by moisture sorption in the case of raw and steam exploded fibres. The successive treatments leading to the exposure of the three hydroxyl groups which is gradually increased from raw fibre to bleached fibre. These hydroxyl groups are tightly bound by intermolecular hydrogen bonding which gives a reduced moisture absorption in the final crystalline cellulose fibre. Acid hydrolysed fibre gives the similar spectra of the bleached fibre since their chemical compositions are identical. In addition, due to the presence of functional groups such as methoxyl–O–CH<sub>3</sub>, C–O–C and aromatic C=C, peaks in the region between 1250 and 1600 cm<sup>-1</sup> was observed (Lojewska et al., 2005; Reddy & Yang, 2005) in the raw and steam exploded fibre. But the destruction of the lignin–cellulose complex (Allinson & Osbourn, 2009) during alkali treatment and bleaching steps facilitate the hydrogen bonding by enhancing the cellulose–cellulose interaction. The increased intensity of the peak at 1000 cm<sup>-1</sup> and the appearance of the new peak at 1320 cm<sup>-1</sup> are due to the isolated cellulose components. From the FTIR analysis it has been concluded that there is a reduction in the quantum of binding components present in the fibres due to the process of steam and chemical treatment. The raw fibres have a characteristic peak in between 1240 and 1740 and at 1240 cm<sup>-1</sup>. These peaks are mainly due to the hemicellulose and lignin components.

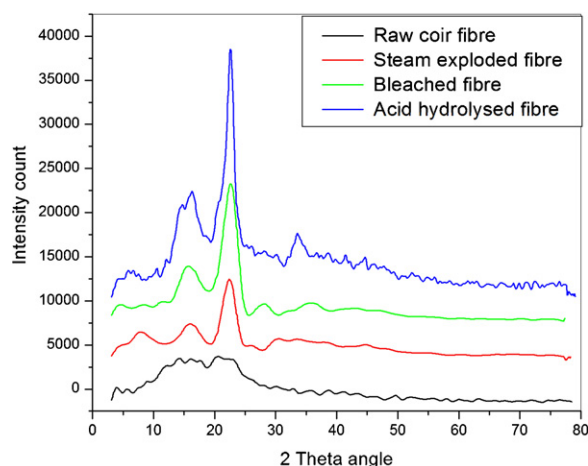


Fig. 2. XRD analysis of coir fibre.

### 3.3. X-ray diffraction analysis

Fig. 2 shows the X-ray diffraction analysis of the coir fibre at various processing stages. The effect of steam explosion coupled with alkali and acid treatments on the fibre structure is clearly envisaged by XRD. In raw fibre, crystalline cellulose components are embedded in the matrix of lignin, hemicellulose, pectin etc. During alkali treatment, the matrix materials react with sodium hydroxide and get start to dissolve along with the formation of traces of the sodium salt of the cellulose. The steam explosion will facilitate the ease of access of the alkali in to the inner part of the raw coir by defibrillation of the fibre. More over it will lead to the swelling of the fibre and subsequent increase in the reacting surface area of the fibre. Alkalization of plant fibres changes the surface topography of the fibres and their crystallographic structure. From the figure it is clear that the raw coir fibre has almost zero crystalline nature and the crystallinity keeps on increasing gradually with processing stages. The zero crystallinity of the raw fibre reveals that each crystalline cellulose components embedded with amorphous lignin components and upon the gradual removal of the lignin by various treatments, the cellulose components tend to form an ordered arrangement. Treatment of the fibres with 2% alkali and successive bleaching processes removed the lignin completely. During the bleaching step, the lignin will dissolve out as lignin chloride and the cellulose component will leave without intact. The final cellulose component has two crystalline peaks, the first at  $2\theta$  value of 10 and the other at  $2\theta$  value of 22. These are the characteristic peaks of cellulose components isolated from natural fibres.

As can be seen, the overall shape of all diffraction patterns is quite similar except untreated raw coir fibre. The baseline of the raw coir fibre diffraction pattern is almost flat, suggesting a higher content of amorphous material in the sample. On removing the noncrystalline constituents (lignin & hemicellulose) from the fibres by chemical treatment, the degree of crystallinity and crystallinity index will change with a positive shift. Other researchers have noted an improvement in the order of the crystallites as the cell wall thickens upon alkali treatment (Nishiyama, Langan, & Chanzy, 2002). Degree of crystallinity of the fibre goes on increasing in both the processing stages. This may be due to the removal of lignin which acts as a cementing material and on delignification, an ordered arrangement of the crystalline cellulose in the structure takes place. By successive experiments, we found that an optimum 10% oxalic acid is fine at the acid hydrolysis step to get a dispersion of cellulose in nanometre dimension. It has been concluded from the X-ray diffractograms that as the raw coir fibres undergo steam

explosion, bleaching and further acid hydrolysis there is a decrease in the fibre diameter as well as an increase in the crystallinity.

### 3.4. Morphological analysis by SEM and SPM

Fig. 3 shows the SEM micrograph of the coir fibre at different processing stages. Fig. 3(A) shows the SEM micrograph of the untreated raw coir fibre. The fibre surface appears to be smooth due to the presence of waxes and oil. However, the presence of pores could be observed on the surface. Though coir fibre has high lignin content (49.2), the moisture absorption capability is comparable (9.2%) with the other fibres. Fig. 3(B) is the alkali treated fibre. The arrangement of cellulose fibres within the matrix of lignin is clearly seen in this picture. The removal of cementing materials, primarily lignin, from the surface of the raw fibre occurs during this step. Fig. 3(C) represents the SEM of fibres subjected to steam treatment after alkali treatment. During the steam explosion with alkali, the hemicellulose is hydrolyzed and become water soluble. The steam explosion facilitates the ease of access of alkali to the interior part of the fibre. The clear demonstration of the defibrillation by steam explosion is seen in this figure. Fig. 3(D) shows the SEM micrograph of the bleached coir fibre. The lignin gets depolymerized and dissolved out at this step which is evident from the chemical analysis. As a result, defibrillation of the fibre occurs because of the removal of the cementing materials which can be seen from the SEM micro photograph.

Bleached fibre is composed of several microfibrils with diameters in the range of 3–12  $\mu\text{m}$ . Each elementary fibre shows a compact structure; exhibiting an alignment in the fibre axis direction with some non-fibrous components in the fibre surface (Garcia-Jaldon, Dupeyre, & Vignon, 1998). It was previously shown that during the chemical treatment (alkalization) most of the lignin and hemicellulose were removed. Mechanical treatment (Steam explosion) further removed the amorphous materials (lignin, hemicellulose, tannin, pectin etc.) from the inner part of the fibre via depolymerisation and defibrillation. Lignin is rapidly oxidized by bleaching agent. Lignin oxidation leads to lignin degradation and thereby to the formation of hydroxyl, carbonyl and carboxylic groups, which facilitate the lignin solubilization in an alkaline medium (Lawther & Sun, 1996). Fibre diameter was again reduced in the acid hydrolysis followed by steam explosion process and cellulose fibre with a diameter of less than 100 nm was obtained. Thus cellulose microfibrils of the original fibres were separated from each other to produce fibrils with diameters around 5–50 nm. The scanning probe microscopy (SPM) image of the final nanocellulose is shown in Fig. 4. The nanofibres are separated in this height image since the sample was subjected to sonication just before the experiment was conducted to avoid the agglomeration. The fibres are dispersed randomly and are white in colour. SPM pictures show the final cellulose nano fibrils with diameters of 5–10 nm which supports the evidence for the isolation of individual nanofibres from raw coir fibre. Acid hydrolysis of cellulose leads to hydrolytic cleavage of glycosidic bond between two anhydroglucose units. Thus the amorphous portion gets dissolved by acid hydrolysis, leaving behind the crystalline regions. Acid hydrolysis followed by mechanical treatment (sonication) results in disintegration of the cellulose structure into nanocrystalline form (Abraham et al., 2011). To calculate the yield of the product formed we have found that 234 g of dry nanocellulose is obtained from 1 kg of dry raw coir fibre.

### 3.5. Dynamic light scattering (DLS) and zeta potential

Dynamic light scattering is one of the most popular light scattering techniques because it allows particle sizing down to 1 nm dimension. Typical applications are emulsions, micelles, polymers,



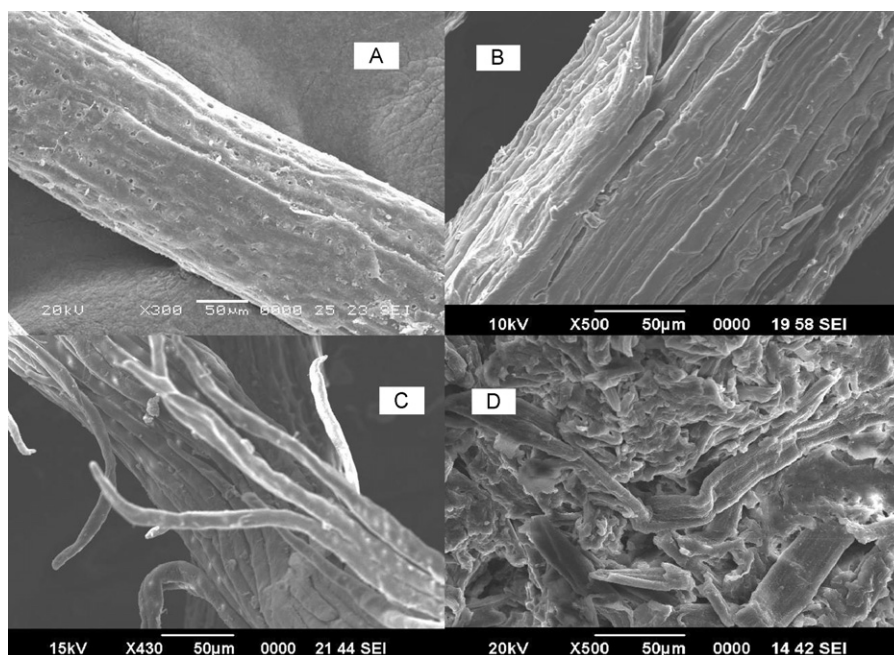


Fig. 3. SEM pictures: (A) raw coir fibre, (B) alkali treated coir fibre, (C) steam exploded coir fibre and (D) bleached coir fibre.

proteins, nanoparticles or colloids. For particle size distribution, the water suspended nanocellulose particles were diluted appropriately and analysed in DLS particle size analyzer. The intensity of light scattered in a particular direction by dispersed nanocellulose tends to periodically change with time. These fluctuations in the intensity vs. time profile are caused by the constant changing of nanocellulose positions brought on by Brownian motion. DLS instruments obtain, from the intensity counts vs. time profile, a correlation function. This exponentially decaying correlation function is analysed for characteristic decay times, which are related to diffusion coefficients and then by the Stokes–Einstein equation, to a particle radius. The physical mechanism that is used to stabilize most aqueous nanocellulose particles systems is electrostatic repulsion. Gaussian size distribution of water suspended nanocellulose particles is given in Fig. 5. The result confirmed the dimension of the nanocellulose particles are in the range of 4–100 nm with

an average value of 37.8 nm. The standard deviation for the particle sizing is 2.1 nm (5.5%) with a *Chi Squared* of 2.114 for Gaussian summary. The linearity in particle size reduction is observed for dilute solution. The increase in the concentration of the suspension resulted in partial agglomeration. The colloidal nanocellulose particles of interest are charged, resulting in their mutual repulsion at extended distances. Ideally, the repulsive forces are sufficiently strong to prevent the nanocelluloses from diffusing close to each other, where short-range van der Waals attractive forces dominate and lead to agglomeration.

Zeta potential is due to the formation of the electric double layer between a solid substrate and a liquid electrolyte. Here it is a measure of the mobility distribution of the dispersion of charged nanocellulose particles as they are subjected to an electric field. The average zeta potential of nanocellulose prepared by acid hydrolysis is  $-18.3$  mV. Zeta potential measured as function of concentration of original aqueous coir nanocellulose suspension in 0.1 mM KCl electrolyte is shown in Fig. 6. Concern is that changing the electrolyte concentration with dilution may have also affected the results. It does appear that using a concentration of between 10 and 20% appears most promising for measuring zeta potential  $f$  (pH) tests. The negative charge on the surface of nanocellulose prepared

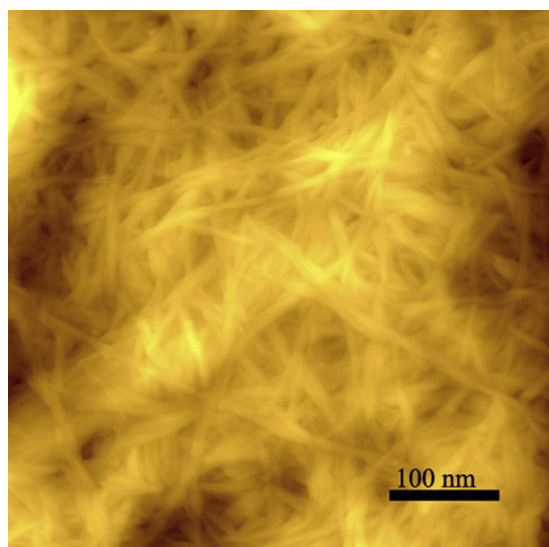


Fig. 4. SPM of cellulose nano dispersion.

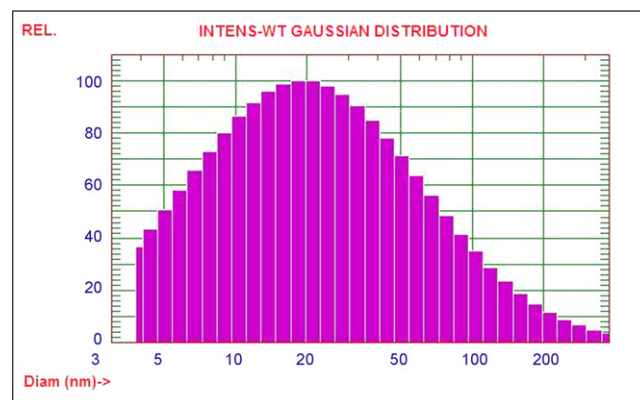


Fig. 5. Gaussian distribution curve of nanocellulose fibre obtained from coir fibre.

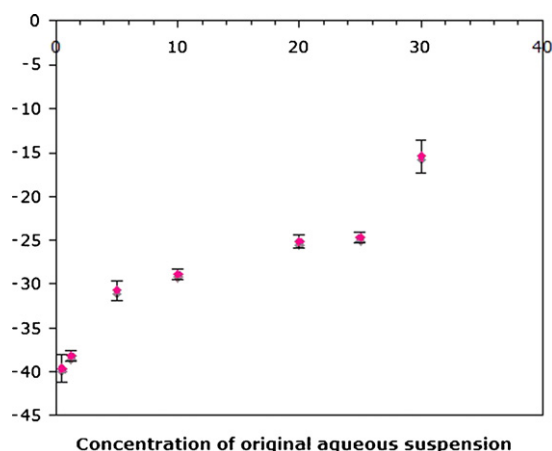


Fig. 6. Zeta potential as a function of concentration (%) of coir nanocellulose suspension in 0.1 mM KCl electrolyte.

by mild oxalic acid hydrolysis indicates the attachment of oxalate groups on its surface. The cellulosic surfaces generally show bipolar character with prevalent acidic contribution due to the proton of the hydroxyl functional group as well as of present carboxyl groups from oxalic acid.

### 3.6. Thermo gravimetric analysis

Thermal decomposition parameters were determined from the DTG curves as described below at a heating rate of 10 °C/min. The DTG curves of the raw coir fibre and the nanocellulose extracted from it are shown in Fig. 7. In the present study, decomposition of the untreated coir fibre shows several stages, indicating the presence of different components that decompose at different temperatures. Due to the differences in the chemical structures between lignin, cellulose and hemicellulose they usually decompose at different temperatures. In both cases, a small weight loss was found in the range of 40–120 °C due to the evaporation of water or low molecular weight compounds. In the case of cellulose nanofibres, the moisture-loss peak shifted to a lower temperature. This tendency towards releasing moisture at a lower temperature might be caused by an increase in the surface area of the split fibres, facilitating easier evaporation of moisture at a lower temperature. The decrease in percentage moisture loss in the nanocellulose could be the effect of increased crystallinity, as observed with X-ray diffraction. The onset temperature for degradation of raw coir

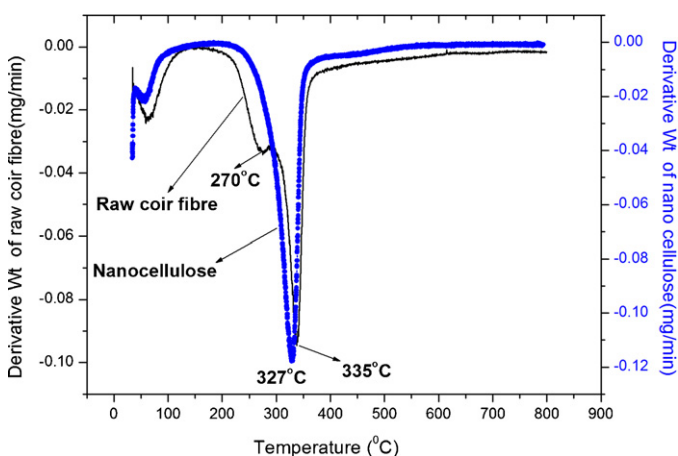


Fig. 7. DTG of raw coir and nanocellulose fibre.

and nanocellulose is 241 °C and 255 °C respectively. The DTG shows the coir fibre with the degradation of lignin, its major cementing material, at a temperature of 270 °C and the  $\alpha$ -cellulose component degrades at 335 °C. Lignin starts its thermal decomposition at 270 °C and persists until 500 °C. It has been observed that the percentage of the solid residue left after the degradation of the raw coir is higher than the percentage weight of the solid residue left after the pyrolysis of the nanocellulose which is extracted from coir fibre. Degree of polymerization of hemicellulose and lignin are very low when compared with cellulose. The higher amount of residual char for raw coir is due to the strong cellulose–lignin complex and the aromatic nature of the lignin complexes. Lignin starts its decomposition at 220 °C and continues up to 300 °C. The decomposition peak reach the maximum mass loss (30 c) at 270 °C, showing a 65 wt.% of solid residuals at 300 °C. Actually, the lignin decomposition extends to the whole temperature range, starting well below 200 °C and persisting above 500 °C. The wide temperature range observed during lignin decomposition is due to the different activities of the chemical bonds present on its structure (Klemm et al., 2004). Here the degradation of extracted nano cellulose has a lower value, 327 °C, than the  $\alpha$ -cellulose embedded in the raw coir fibre (335 °C). This reduction in the degradation temperature is due to the presence of strong lignin–cellulose complex which exist in raw coir fibre. Raw coir fibre has a lignin content of 45–50% of weight. Lignin has an aromatic skeletal structure and the cellulose and lignin are packed in the raw coir as a lignin–cellulose complex which is more thermally stable than pure  $\alpha$ -cellulose. This is reflected in the increased amount of residual char. This lignin–cellulose complex can be believed to protect the  $\alpha$ -cellulose from degradation to a considerable extent. An increase in residual char formation and lowering of the degradation temperature during the pyrolysis of treated cotton has also been reported (Garcia-Jaldon et al., 1998; Hinojosa, Arthur, & Mares, 1973; Lawther & Sun, 1996; Paul et al., 2008). It might be caused by an increased rate of formation of free radicals that are stabilized by condensed carbon ring formations in the char (Hinojosa et al., 1973). The percentage degradation remain almost the same for the  $\alpha$ -cellulose but decrease for lignin, confirming the observation that >45% lignin was removed by the treatment. At 400 °C almost all cellulose was pyrolyzed, and the solid residual char for nanocellulose is 22.53 wt.% at 600 °C. This value of residual char is little lower than the cellulose together with lignin in the raw coir (26.29 wt.%). The residual char left at 600 °C decreased considerably from 26.29 to 22.53% in the case of nanofibres. A similar observation was reported by Saha, Ray, Pandey, & Goswamy (1991) who explained that alkali treatment followed by steam explosion removed the lignin to a considerable extent, reduced the strength of lignin–cellulose complex, thereby making the product less stable than the raw sample, and this was reflected in the decreased amount of residual char. Thus generally nano celluloses obtained from coir fibre has lower thermal stability than the  $\alpha$ -cellulose present in the untreated coir fibres. In addition, they showed lower amounts of residual solids.

In the first half of the degradation process (30–300 °C) nanocellulose shows higher thermal stability than raw fibre and in the second half (300–600 °C) later has higher thermal stability. An increase in residual char formation and the degradation temperature for raw coir during the pyrolysis may be due to the increased rate of formation of free radicals at higher temperature that are stabilized by condensed carbon ring formations in the char (Jawaid & Abdul Khalil, 2011). Nanocellulose extracted from raw fibre shows reduced pyrolysis temperature, increased weight loss during pyrolysis, and reduced residual char formation with a lowering in the formation of the flammable volatiles, and thus it can be easily concluded that the thermal stability of  $\alpha$ -cellulose embedded in raw coir shows increased thermal stability than the  $\alpha$ -cellulose extracted from it.

#### 4. Conclusion

The objective of this work was to extract nanocellulose from raw coir fibre and thereby enhance its effective utilization and to avoid the retting process of the coir fibre which makes strong environmental problems. Steam explosion has been found to be successful in obtaining fibres in the nano dimension from raw coir fibres. The presence of lignin–cellulose complex in the raw coir fibre plays a major role in its structural and thermal properties of the fibre. The thermal stability of the extracted nanocellulose has a lower value than the nanocellulose present in the raw coir fibre because of the presence of this strong lignin–cellulose complex in raw fibre. Homogenous cellulose nanofibrils with a diameter of 5–50 nm are obtained from coir fibre by this process. Since the pure cellulose has a variety of properties, its nano form can find applications in various industrial and biomedical fields by exploring the nanotechnological possibilities (Abraham et al., 2011; Goetz et al., 2009; Zimmermann et al., 2004).

#### Acknowledgements

The authors are grateful to the Department of Science and Technology (DST), Government of India, for the financial funding of this research work and Mr. Abraham Mathew for providing the coir fibre.

#### References

- Abraham, E., Deepa, B., Pothan, L. A., Jacob, M., Thomas, S., & Anandjiwala, R. (2011). Extraction of nanocellulose fibrils from lignocellulosic fibres: A novel approach. *Carbohydrate Polymers*, 86, 1468–1475.
- Allinson, D. W., & Osbourn, D. F. (2009). The cellulose–lignin complex in forages and its relationship to forage nutritive value. *The Journal of Agricultural Science*, 74, 23–36.
- Ayrilmis, N., Jarusombuti, S., Fueangvivat, V., Bauchongkol, P., & White, R. H. (2011). Coir fiber reinforced polypropylene composite panel for automotive interior applications. *Fibers and Polymers*, 12, 919–926.
- Erdtman, H. (2003). Lignins: Occurrence, formation, structure and reactions. *Journal of Polymer Science, Part B: Polymer Letters*, 10, 228–230.
- Garcia-Jaldon, G., Dupeyre, D., & Vignon, M. R. (1998). Fibres from semi-retted hemp bundles by steam explosion treatment. *Biomass and Bioenergy*, 14, 251–260.
- Geethamma, V. G., Thomas Mathew, K., Lakshminarayanan, R., & Thomas, S. (1998). Composite of short coir fibres and natural rubber: Effect of chemical modification loading and orientation of fibre. *Polymer*, 39, 1483–1491.
- Goetz, L., Mathew, A., Oksman, K., Gatenholm, P., & Ragauskas, A. J. (2009). A novel nanocomposite film prepared from crosslinked cellulosic whiskers. *Carbohydrate Polymers*, 75, 85–89.
- Hinojosa, O., Arthur, J. C., & Mares, T. (1973). Thermally initiated free-radical oxidation of cellulose. *Textile Research Journal*, 43, 609.
- Hon, D. N.-S. (1994). Cellulose: a random walk along its historical path. *Cellulose*, 1, 1–25.
- Itoh, T., Jr., & Brown, R. M. (1984). The assembly of cellulose microfibrils in *Valonia macrophysa*. *Journal of Cell Biology*, 160, 372–381.
- Jawaid, M., & Abdul Khalil, H. P. S. (2011). Cellulosic/synthetic fibre reinforced polymer hybrid composites: A review. *Carbohydrate Polymers*, 86, 1–18.
- Klemm, D., Philipp, B., Heinze, T., Heinze, U., & Wagenknecht, W. (2004). General considerations on structure and reactivity of cellulose: Section 2.4–2.4.3. In *Comprehensive Cellulose Chemistry*. Wiley-VCH Verlag GmbH, 130–165.
- Klemm, D., Schumann, D., Kramer, F., Hebler, N., Hornung, M., & Marsch, S. (2006). Nanocelluloses as innovative polymers in research and application. *Advanced Polymer Science*, 205, 49–96.
- Lawther, J. M., & Sun, R. (1996). The fractional characterisation of polysaccharides and lignin components in alkaline treated and atmospheric refined wheat straw. *Industrial Crops and Products*, 5, 87–95.
- Lojewski, J., Miskowicz, P., Lojewski, T., & Pronienicz, L. M. (2005). Cellulose oxidative and hydrolytic degradation: in situ FTIR approach. *Polymer Degradation & Stability*, 88, 512–520.
- Mohanty, A. K., Misra, M., & Hinrichsen, G. (2000). Biofibres, biodegradable polymers and biocomposites: An overview. *Macromolecular Materials & Engineering*, 276/277, 1–24.
- Narayanan, P. I. (1999). *Development of microbial treatment of ret liquor generated in a coir retting bioreactor*; Ph D thesis, School of Environmental Studies; Cochin University of Science and Technology (CUSAT), Kerala, India.
- Nishiyama, Y., Langan, P., & Chanzy, H. (2002). Crystal structure and hydrogen-bonding system in cellulose I $\beta$  from synchrotron X-ray and neutron fiber diffraction. *Journal of American Chemical Society*, 124, 9074–9082.
- Oh, S. Y., Yoo, D. I., Shin, Y., & Seo, G. (2005). FTIR analysis of cellulose treated with sodium hydroxide and carbon dioxide. *Carbohydrate Research*, 340, 417–428.
- Paul, S. A., Piasta, D., Spange, S., Pothan, L. A., Thomas, S., & Bellmann, C. (2008). Solvatochromic and electrokinetic studies of banana fibrils prepared from steam-exploded banana fiber. *Biomacromolecules*, 9, 1802–1810.
- Reddy, N., & Yang, Y. (2005). Structure and properties of high quality natural cellulose fiber from cornstalks. *Polymer*, 46, 5494–5500.
- Saha, S. C., Ray, P. K., Pandey, S. N., & Goswamy, K. (1991). IR and X-ray diffraction studies of raw and chemically treated pineapple leaf fiber (PALF). *Journal of Polymer Science*, 42, 2767–2772.
- Zimmermann, T., Pohler, E., & Geiger, G. (2004). Cellulose fibrils for polymer reinforcement. *Advanced Engineering Materials*, 6, 754–761.